

# Infrared Molecular Starburst Fingerprints in Deeply Obscured (U)LIRG Nuclei

F. Lahuis<sup>1,2</sup>, H. W. W. Spoon<sup>3,4</sup>, A. G. G. M. Tielens<sup>5</sup>, S. D. Doty<sup>6</sup>, L. Armus<sup>7</sup>,  
 V. Charmandaris<sup>8,9</sup>, J. R. Houck<sup>3</sup>, P. Stäuber<sup>10</sup>, & E. F. van Dishoeck<sup>1</sup>

F.Lahuis@sron.rug.nl

## ABSTRACT

High resolution spectra of the *Spitzer* Space Telescope show vibration-rotation absorption bands of gaseous C<sub>2</sub>H<sub>2</sub>, HCN, and CO<sub>2</sub> molecules toward a sample of deeply obscured (U)LIRG nuclei. The observed bands reveal the presence of dense ( $n \gtrsim 10^7 \text{ cm}^{-3}$ ), warm ( $T_{\text{ex}} = 200 - 700 \text{ K}$ ) molecular gas with high column densities of these molecules ranging from a few  $10^{15} - 10^{17} \text{ cm}^{-2}$ . Abundances relative to H<sub>2</sub>, inferred from the silicate optical depth, range from  $\sim 10^{-7}$  to  $10^{-6}$  and show no correlation with temperature. Theoretical studies show that the high abundances of both C<sub>2</sub>H<sub>2</sub> and HCN exclude a X-ray dominated region (XDR) associated with the toroid surrounding an AGN as the origin of this dense warm molecular gas. Galactic massive protostars in the so-called Hot Core phase have similar physical characteristics with comparable high abundances of C<sub>2</sub>H<sub>2</sub>, HCN, and CO<sub>2</sub> in the hot phase. However, the abundances of C<sub>2</sub>H<sub>2</sub> and HCN and the C<sub>2</sub>H<sub>2</sub>/CO<sub>2</sub> and HCN/CO<sub>2</sub> ratios are much higher toward the (U)LIRGs in the cooler ( $T_{\text{ex}} \lesssim 400 \text{ K}$ ) phase. We suggest that the

---

<sup>1</sup>Leiden Observatory, P.O. Box 9513, 2300 RA Leiden, The Netherlands

<sup>2</sup>SRON Netherlands Institute for Space Research, P.O. Box 800, 9700 AV Groningen, The Netherlands

<sup>3</sup>Cornell University, Astronomy Department, Ithaca, NY 14853

<sup>4</sup>*Spitzer* Fellow

<sup>5</sup>MS 245-3, NASA Ames Research Center, Moffett Field, CA 94035

<sup>6</sup>Department of Physics and Astronomy, Denison University, Granville, OH 43023, USA

<sup>7</sup>Caltech, *Spitzer* Science Center, MS 220-6, Pasadena, CA 91125

<sup>8</sup>Department of Physics, University of Crete, GR-71003, Heraklion, Greece

<sup>9</sup>IESL / Foundation for Research and Technology- Hellas, PO Box 1527, GR-71110, Heraklion, Greece, and Chercheur Associé, Observatoire de Paris, F-75014, Paris, France

<sup>10</sup>Institute of Astronomy, ETH-Zentrum, 8092 Zurich, Switzerland

warm dense molecular gas revealed by the mid-IR absorption lines is associated with a phase of deeply embedded star formation where the extreme pressures and densities of the nuclear starburst environment have inhibited the expansion of HII regions and the global disruption of the star forming molecular cloud cores, and ‘trapped’ the star formation process in an ‘extended’ Hot Core phase.

*Subject headings:* infrared: ISM – ISM: evolution – ISM: galaxies – ISM: molecules – galaxies: nuclei

## 1. Introduction

One of the holy grails in the study of luminous and ultraluminous infrared galaxies (LIRGs and ULIRGs) is to elucidate the true nature of the central energy source. (U)LIRGs emit nearly all their energy in the mid and far-infrared part of the spectrum. LIRGs have a luminosity  $L_{8-1000\mu\text{m}} > 10^{10}L_\odot$  and ULIRGs  $L_{8-1000\mu\text{m}} > 10^{12}L_\odot$ , equal to the power output of quasars. (U)LIRGs are generally found in interacting and merging systems (e.g. Armus, Heckman, & Miley 1987; Sanders et al. 1988a; Murphy et al. 1996). During the merger large amounts of gas and dust are concentrated toward the nucleus (e.g. Mihos & Hernquist 1996), fueling a massive starburst and possibly a massive black hole (an AGN). (U)LIRGs are without doubt the most spectacular sites of star formation in the Universe and if a substantial part of their energy originates from AGN activity, it would show the AGN in its very earliest deeply enshrouded phase.

The sensitive Infrared Spectrograph (IRS) (Houck et al. 2004) on board the *Spitzer* Space Telescope (Werner et al. 2004) has revealed the richness, complexity and diversity of the mid-infrared spectra toward a sample of deeply obscured (U)LIRGs (Armus et al. 2004, 2006a,b; Spoon et al. 2006a,b); see Genzel & Cesarsky (2000) for a review of results from the Infrared Space Observatory. The general characteristic of these spectra is the presence of deep, broad absorption of amorphous silicates, centered at 10 and 18  $\mu\text{m}$ . In addition, the spectra show a large variety in absorption features of crystalline silicates, aliphatic hydrocarbons, water ice, and gas phase bands of hot CO (Spoon et al. 2004, 2006c). PAH emission bands are generally weak and in some cases absent. Absorption bands of more volatile ices (e.g. CO or CO<sub>2</sub>), commonly detected in Galactic dense molecular clouds, are generally absent or very weak.

The very compact nuclei of deeply obscured (U)LIRGs are packed with gas. Molecular gas has been observed at millimeter wavelengths — through its low lying pure rotational transitions — in (U)LIRG nuclei (e.g. Solomon et al. 1997; Downes & Solomon 1998), see Aalto (2005) for a recent overview. In recent years millimeter emission lines of HCN and HCO<sup>+</sup> have been observed revealing the presence of relatively dense ( $n_{\text{H}} \sim 10^5 \text{ cm}^{-3}$ ) molecular gas (Imanishi et al. 2006;

Kohno 2005). However, the analysis of the millimeter emission lines is complicated as a result of beam dilution which strongly depends on the molecules and transitions observed.

The IRS Short-High spectrometer (IRS-SH) on board the *Spitzer* Space Telescope allows for the first time the direct study of the very dense and warm molecular gas in the central regions of deeply obscured luminous and ultraluminous infrared galaxies through IR pencil-beam line-of-sight absorption spectroscopy against the continuum of individual nuclei or unresolved<sup>11</sup> double nuclei. In particular, the mid-infrared vibration-rotation bands of C<sub>2</sub>H<sub>2</sub> and HCN uniquely trace warm ( $100 < T < 1000$  K) and dense ( $n_{\text{H}} > 10^7 \text{ cm}^{-3}$ ) molecular gas. These bands have previously been detected primarily toward Galactic massive protostars (Lacy et al. 1989; Evans et al. 1991; Lahuis & van Dishoeck 2000). They may prove to be a new strong tool to probe the heating sources of deeply obscured (U)LIRG nuclei (starburst or AGN activity).

## 2. Observations

The observations presented in this paper are part of the *Spitzer* IRS observing programs (PID) 105 (IRS GTO ULIRG program, J.R. Houck PI), 96 (IRS GTO program on nearby AGN, J.R. Houck PI) and 1096 (Director's Discretionary Time (DDT) proposal, H.W.W. Spoon PI). The IRS GTO ULIRG sample comprises  $\sim 100$  ULIRGs in the redshift range  $0.02 < z < 0.93$ , selected primarily from the IRAS 2-Jy sample (Strauss et al. 1992), IRAS 1-Jy sample (Kim & Sanders 1998) and the FIRST/IRAS radio-far-IR sample (Stanford et al. 2000). The samples of PIDs 96 and 1096 contain 3 additional ULIRGs (IRAS 04384–4848, IRAS 03000–2719 and IRAS 02113–2937) and 3 additional LIRGs (IRAS 02530+0211, IC 860 and NGC 4418). For all sources in this combined sample low-resolution spectra ( $R = \lambda/\Delta\lambda \sim 100$ ) have been obtained, while high resolution spectra ( $R = 600$ ) have been taken only for the brighter half of the sample.

All high resolution spectra in this sample have been investigated for the presence of vibration-rotation absorption bands of C<sub>2</sub>H<sub>2</sub> (13.7  $\mu\text{m}$ ), HCN (14.02  $\mu\text{m}$ ) and CO<sub>2</sub> (15.0  $\mu\text{m}$ ) against the nuclear continuum. Fifteen of the sources listed in Table 1 show absorption due to (some of) these species. Because of the low signal to noise ratio of the spectra and/or the low H-column densities (as derived from the 9.7  $\mu\text{m}$  silicate optical depth; see Section 3.3), the derived upper limits on the molecular column densities for all other sources do not place very stringent constraints on the C<sub>2</sub>H<sub>2</sub> and HCN abundances. To illustrate this, four sources without positive detections with both a moderate-to-large hydrogen column density and good signal to noise spectra, are included in Tables 1 and 2. The upper limits on the C<sub>2</sub>H<sub>2</sub> and HCN abundances fall within the range of derived

---

<sup>11</sup>The IRS-SH slit width is 4.7", equal to the size of the PSF at 19.5  $\mu\text{m}$ .

abundances toward the fifteen sources.

Data reduction started from crosstalk corrected echelle images using S12 and S13 *Spitzer* archive data. Processing was done using the c2d analysis pipeline (Kessler-Silacci et al. 2006; Lahuis et al. 2006). It includes echelle image analysis (a.o. bad-pixel detection, image arithmetic, and optimal spectral extraction), defringing of the extracted spectra (Lahuis & Boogert 2003), and spectral analysis (see Section 3.1). The optimal spectral extraction uses an analytical source profile defined and calibrated using a suite of calibrator stars. Calibration is done using MARCS stellar models provided by the *Spitzer* Science Center (Decin et al. 2004). The optimal spectral extraction employs a combined source and local sky fit. This provides wavelength dependent sky estimates and allows to discriminate between resolved and unresolved spectral features.

Figure 1 shows the continuum divided, sky and redshift-corrected spectra from 13.5–15.5  $\mu\text{m}$  covering the absorption bands of  $\text{C}_2\text{H}_2$ , HCN and  $\text{CO}_2$ . Plotted in red are the best-fit single temperature synthetic spectra (see Section 3). Indicated with the dotted verticals are the positions of the ground-state *Q*-branch transitions of the three molecules. For IRAS 15250+3609, IRAS 20100–4156, and IC 860 a small section of the spectrum in between HCN and  $\text{CO}_2$  is affected by artifacts in inter-order sections of the spectrum, and these sections have been clipped from the presented spectra.

### 3. Analysis

#### 3.1. Molecular analysis

The *Spitzer* spectra unambiguously reveal the presence of the *Q*-branch transitions of  $\text{C}_2\text{H}_2$   $\nu_5 = 1 - 0$ , HCN  $\nu_2 = 1 - 0$  and  $\text{CO}_2$   $\nu_2 = 1 - 0$ , each of which blends into a "broad" absorption feature. The corresponding *P*- and *R*-branch transitions of these species are difficult to observe with the *Spitzer*-IRS due to spectral dilution at the IRS resolving power and the presence of instrumental fringe residuals with frequencies and amplitudes close to those of the *P*- and *R*-branch lines. The *Q*-branch transitions are analyzed using a pure absorption model assuming local thermodynamic equilibrium (LTE) excitation of the levels at a single temperature. The adopted method is described in detail in Lahuis & van Dishoeck (2000) and Boonman et al. (2003), which includes references to the molecular parameters and data used in the model. The main fit parameters are the excitation temperature and column density along the line of sight for a given intrinsic line width, defined by the Doppler *b*-value. It is assumed that the absorbing molecules have a covering factor of unity of the continuum, i.e. the mid-IR continuum is composed solely by the regions toward which the molecular absorption features arise. A covering factor less than unity, i.e. larger continuum emitting regions, increases the true optical depth of the absorption features resulting in higher

column densities and possibly lower temperatures (when lowest excitation lines saturate at large column densities).

The derived excitation parameters do not strongly depend on the exact value of  $b$ . Only for low values of  $b$  ( $\lesssim 5 \text{ km s}^{-1}$ ) will saturation result in an underestimate of the column density for the sources with the largest column densities. Such low  $b$  values are expected for quiescent gas where thermal broadening dominates. However, non-thermal broadening will likely dominate in the dense energetic ISM of the galactic nuclei and larger  $b$  values are expected.

A direct estimate of  $b$  is obtained from spectrally resolved CO  $\nu = 1 - 0$  absorption lines toward the north-west nucleus of IRAS 08572+3915 (Geballe et al. 2006), which shows a complex velocity structure. A low column density, cold CO component absorbs near the systemic velocity. The CO absorption is however dominated by a broad (FWHM  $\sim 200 \text{ km s}^{-1}$ ) blue-shifted warm ( $\gtrsim 200 \text{ K}$ ) gas component. This is most likely the conglomerate of a velocity distribution over multiple lines of sight within the beam. The continuum confusion then requires a higher column density than that of  $2 \times 10^{18} \text{ cm}^{-2}$  estimated from the observed optical depth by Geballe et al. (2006). We have fitted synthetic LTE absorption spectra to the higher excitation CO lines using the spectrum of Geballe et al. (2006) but with the spectral resolution reduced to match the observed profile width ( $R \sim 1500$ ). This allows to estimate a velocity averaged column density for a given  $b$  value. Values  $< 10 \text{ km s}^{-1}$  result in progressively poorer fits. Good fits are made for  $b$  values of  $10 - 25 \text{ km s}^{-1}$  requiring column densities of  $\sim 2 \times 10^{19} \text{ cm}^{-2}$  down to  $\sim 5 \times 10^{18} \text{ cm}^{-2}$ . The Doppler  $b$ -value has therefore been fixed to  $20 \text{ km s}^{-1}$  for all sources.

Recent observations using TEXES (Lacy et al. 2002), visitor instrument on Gemini-North, have revealed spectrally resolved (FWHM  $\sim 80 \text{ km s}^{-1}$ ) blue-shifted absorption in the C<sub>2</sub>H<sub>2</sub>  $\nu_5 = 1 - 0$  R(13) ro-vibrational line toward one of our sources, NGC 4418 (Knez, private communication). The current data do not allow to put more stringent constraints on the Doppler  $b$ -value. However, the spectrally resolved C<sub>2</sub>H<sub>2</sub> absorption could be an indication that multiple (spatial and velocity) components of the warm and dense gas are common in (U)LIRG nuclei.

### 3.2. Fit results

Table 2 lists the derived excitation temperatures and column densities from best fit synthetic spectra to the continuum divided (U)LIRG spectra. Excitation temperatures ranging from 200 to 700 K and column densities of a few  $\times 10^{15}$  to  $10^{17} \text{ cm}^{-2}$  are observed. These results are derived from a simultaneous fit to the three absorption bands, in which the excitation temperature, set to be the same for all three molecules, is constrained by the  $Q$ -branch profiles of C<sub>2</sub>H<sub>2</sub> and HCN. Since the analysis is restricted to that of the analysis of the resolved  $Q$ -branches (see 3.1), the

derived excitation temperatures are not well constrained ( $\sim 30\%$ ). However it does clearly allow to discriminate between molecular gas with warm ( $\sim 200$ – $300$  K) and hot ( $\sim 500$ – $700$  K) excitation temperatures. This is illustrated in Figure 2 by fits to the observed absorption profiles of IC 860 and IRAS 01003-2238, for which we derive excitation temperatures of 280 and 630 K respectively.

The  $Q$ -branch profiles of  $\text{C}_2\text{H}_2$  and HCN reveal significant contributions to the absorption from relatively high rotational levels. Hence, given the high critical density of these levels, the absorbing gas is likely very dense ( $n \gtrsim 10^7 \text{ cm}^{-3}$ ). Observations of the ro-vibrational transitions of CO in IRAS 08572+3915 and IRAS 00183-7111 indeed imply densities in excess of  $3 \times 10^6 \text{ cm}^{-3}$  (Geballe et al. 2006; Spoon et al. 2004).

### 3.3. Abundances

The derived column densities are translated into abundances by using a total hydrogen column density obtained from the apparent optical depth of the  $9.7\mu\text{m}$  silicate absorption band listed in Table 1. The optical depth is converted assuming:

$$N_{\text{H}} = \tau_{9.7} (3.5 \times 10^{22}) \text{ cm}^{-2},$$

appropriate for the dust in the solar neighbourhood (Roche & Aitken 1984, 1985).

This relation is most appropriate for embedded (extinction dominated) sources probing the absorption along the pencil beam line of sight toward the warm central continuum emitting region. To illustrate, for the sample of Galactic massive protostars (see Section 4.3) the hydrogen column density derived using the silicate optical depth estimated from the ISO-SWS archive spectra agrees within a factor of two with the hydrogen column density derived from CO  $\nu = 1-0$  measurements (Mitchell et al. 1990; Lahuis & van Dishoeck 2000).

Another estimate of the applicability of this method is provided through the analysis of the  $4.6\mu\text{m}$  CO  $\nu = 1-0$  absorption spectrum toward IRAS 08572+3915NW, which gives CO column densities of  $\sim 5 \times 10^{18} \text{ cm}^{-2}$  up to  $\sim 2 \times 10^{19} \text{ cm}^{-2}$  depending on the assumed value of  $b$  (see Section 3.1). Adopting  $N_{\text{CO}}/N_{\text{H}} = 10^{-4}$  (all gas-phase carbon in CO) this results in  $N_{\text{H}} = 5 \times 10^{22} - 2 \times 10^{23} \text{ cm}^{-2}$ . This is in reasonable agreement with the hydrogen column density derived from the silicate optical depth ( $N_{\text{H}} \sim 1.5 \times 10^{23} \text{ cm}^{-2}$ ). If anything, the IRAS 08572+3915NW data suggest the hydrogen column density might be slightly overestimated (e.g. as a result of foreground extinction) resulting in underestimating the derived molecular abundances. We assume a similar uncertainty for the other sources.

The derived abundances and  $\text{H}_2$  column densities (assuming  $N_{\text{H}_2} = N_{\text{H}}/2$ ) are listed in Table 2. The HCN abundance is up to three orders of magnitude higher than in cold molecular clouds

(Bergin & Langer 1997). High abundances of HCN, C<sub>2</sub>H<sub>2</sub>, and CO<sub>2</sub> have also been measured for Galactic massive protostars (see Section 4.3). Figures 3 and 4 compare the abundances to chemical models and results from studies of Galactic massive young stellar objects (Section 4).

### 3.4. Gas temperature

The derived excitation temperatures range from 200 to 700 K. While statistics are small, of the seven sources with the highest gas excitation temperatures ( $T_{\text{ex}} = 400\text{--}700\text{ K}$ ) five sources show the highest 5.5  $\mu\text{m}$  to 28  $\mu\text{m}$  continuum flux ratio. These galaxies also show a rising near-IR continuum typical for hot dust while the other galaxies show a decreasing near-IR continuum characteristic for emission dominated by stellar photospheres. It seems thus that there is a connection between the observed dust and molecular excitation temperatures.

The presence of absorption (rather than emission) lines implies a strong gradient in the temperature and an underlying hot-dust continuum against which the absorption lines are formed. However, the derived excitation temperatures of the molecular gas for the warmest sources ( $T_{\text{ex}} = 400\text{--}700\text{ K}$ ) are higher by a factor of 2 to 3 than the mid-IR color temperature derived from the 5.5 to 28.0  $\mu\text{m}$  flux ratio. While the discrepancy between the excitation temperatures and the mid-IR color temperature may (in part) reflect the uncertainties in the analysis, the observed colder dust continuum may point towards the importance of continuum extinction by (a shell of) colder foreground dust exterior to the C<sub>2</sub>H<sub>2</sub> and HCN absorbing layer, or the predominance of emission of cold nuclear dust within the IRS aperture (i.e. a small beam filling factor for the warm dust and gas). Both may result in an added uncertainty in the derived abundances resulting from overestimating the hydrogen column density or from a covering factor of the molecule rich warm gas less than unity (see Section 3.1).

## 4. Discussion

### 4.1. Warm molecular gas in (U)LIRGs

The *Spitzer*-IRS spectra reported here reveal surprisingly strong mid-IR absorption bands of C<sub>2</sub>H<sub>2</sub>, HCN and CO<sub>2</sub> toward a sample of (U)LIRG nuclei. These absorptions reveal the presence of copious amounts of warm molecular material and are in line with earlier detections of warm CO gas (Spoon et al. 2004, 2006a; Geballe et al. 2006). This molecular gas is very dense ( $n \gtrsim 3 \times 10^6\text{ cm}^{-3}$ ) and warm ( $T \sim 200\text{--}700\text{ K}$ ). Given the column density and estimated density, this gas occupies only a small fraction of the nuclear region ( $\sim 0.01\text{ pc}$ ) and, given its high temperature, is

likely located near the intrinsic mid-infrared source of luminosity of these regions.

At present there are still substantial uncertainties in accurately inferring the nature of the power source dominating the bolometric luminosity in infrared luminous galaxies. As discussed in Armus et al. (2006b), it appears that there are disagreements among various diagnostic diagrams based on line ratios, continuum colors or PAH equivalent width. Perusal of the 2–40 $\mu$ m spectra reveal that the sources with molecular gas absorptions appear to be a “mixed bag”. While most sources show a deep silicate feature, some (e.g., Mrk231, IRAS 01003-2238, IRAS 05189-2524 and IRAS 13218+0552) do not. Indeed, the 2–40 $\mu$ m continuum spectra of these sources show strong similarities with the spectra of bona fide AGN-dominated spectra with shallow silicate features. In contrast, sources like IRAS 17208-0014 and IRAS 22491-1808 look quite starburst-like. Finally, sources such as IRAS 08572+3915 show neither signs of starburst activity (e.g., PAH features) nor signs of AGN activity (e.g., high ionization lines or a broad H $\alpha$  line). While the presence of hot dust, as visible in the near-IR, may be taken as evidence for the presence of an embedded AGN in this source, any deeply obscured source – including deeply embedded protostars – will produce hot dust. Indeed, the overall mid-IR spectrum of IRAS 08572+3915 resembles that of many galactic massive protostars, such as AFGL 2591, with a preponderance of dust absorption features.

The C<sub>2</sub>H<sub>2</sub>, HCN, and CO<sub>2</sub> molecular lines may provide a new probe of the conditions in the inner deeply obscured nuclei and hence shed light on the ultimate power source of (U)LIRGs; e.g., starburst phenomena versus AGN activity. In particular, the presence of copious amounts of warm molecular gas enriched in C<sub>2</sub>H<sub>2</sub>, HCN, and CO<sub>2</sub> is common in regions of massive star formation (Boonman et al. 2003; Lahuis & van Dishoeck 2000; Lacy et al. 1989; Evans et al. 1991), while, on the other hand, X-rays associated with a central black hole can influence molecular chemistry and abundances far beyond the mean free path length of stellar (E)UV photons. The molecular observations are discussed in the light of these scenarios in the next subsections. While the possible errors associated with the derived abundances are recognized, the discussion will center on Figures 3 and 4.

## 4.2. AGN activity and X-ray driven chemistry

Sub-millimeter studies have revealed high HCN/CO (and HCN/HCO<sup>+</sup>) abundance ratios in Seyfert type I nuclei and this has been taken as an indication of the importance of X-ray illumination for the composition of the molecular gas in these nuclei (Imanishi et al. 2006; Kohno 2005). Some of the sources in our sample are known to harbor an AGN. In particular, Mrk 231 and IRAS 13218+0552 are QSOs, IRAS 08572+3915 and UGC 5101 are LINERs, and IRAS 01003-2238, IRAS 05189-2524 and Mrk 273 have optical LINER/Seyfert 2 spectra (see Table 1). Hence,

the observed high abundance of HCN, and by inference C<sub>2</sub>H<sub>2</sub> (which has no pure rotational transitions), may indicate the presence of a buried AGN in all of our sources. The complex geometry and inhomogeneous dust distribution associated with the central toroid may then preclude our detection of the putative X-rays photons from the central engine driving the chemistry of the molecular gas. The mid-IR observations presented in this paper add to the submillimeter results the predominance of *warm* molecular gas. Within the AGN heating scenario, it seems obvious to attribute the high temperature of the molecular gas to the importance of X-ray heating in a so-called XDR (Maloney et al. 1996; Meijerink & Spaans 2005). Alternatively Gao & Solomon (2004) argue that most (U)LIRGs are dominated by starburst power rather than AGN power based on the HCN  $J = 1 - 0$  luminosity and CO  $J = 1 - 0$  luminosity relation. In a starburst scenario the HCN/CO ratio traces the amount of dense molecular gas in the galactic ISM. Our observations may present an additional test for these two scenarios.

X-rays are not only an efficient heating agent of the gas but also have a major influence on the chemical composition. This has been explored in the context of AGNs by Maloney et al. (1996); Meijerink & Spaans (2005), and for regions around protostars by Stäuber et al. (2005, 2006). At the high densities relevant for these regions, the gas temperature is set by a balance between X-ray heating and gas-dust collisional cooling. As an example, a gas temperature of 200 K at a density of  $\sim 3 \times 10^6$  cm<sup>-3</sup> requires a X-ray flux of  $\sim 30$  erg cm<sup>-2</sup> s<sup>-1</sup> which for a typical Seyfert galaxy with an X-ray luminosity of  $10^{44}$  erg s<sup>-1</sup> corresponds to a distance of 50 pc for an unobscured view of the central engine. For the molecular features to be seen in absorption, the mid-IR continuum has to arise from an inner, warmer zone (e.g., exposed to a higher X-ray flux). Since most of these (U)LIRGs show no evidence for strong X-ray emission while the column density associated with the molecular gas ( $10^{22} - 10^{23}$  cm<sup>-2</sup>) is small compared to X-ray attenuation lengths, in this AGN-scenario, the direct view of the nucleus would have to be blocked by a high-column-density, edge-on toroid while the warm molecular gas is offset to the polar regions and has a little-obstructed view of the nucleus.

An AGN origin for the high abundance of warm HCN, C<sub>2</sub>H<sub>2</sub>, and CO<sub>2</sub> in these (U)LIRGs however faces severe theoretical difficulties. Specifically, the high X-ray flux required to explain the observed temperatures readily dissociates the molecules and drives the gas atomic (Maloney et al. 1996; Meijerink & Spaans 2005). Indeed, calculated HCN abundances are typically less than 10<sup>-8</sup> wrt. H in X-ray illuminated gas while C<sub>2</sub>H<sub>2</sub> is virtually destroyed for X-ray fluxes in excess of 1 erg cm<sup>-2</sup> s<sup>-1</sup>. This is illustrated in Figure 3 which presents the static steady-state chemical composition after equilibrium is reached ( $\sim 10^5$  yr) for clouds illuminated by X-rays. Here, static means that the chemistry has been evolved in time – while the X-ray flux, temperature, and density are fixed – until steady state is achieved in the chemical abundances (see also Stäuber et al. 2005, 2006). The X-ray spectrum is assumed to be thermal in nature with  $T_X = 3 \times 10^7$  K. The chemistry is relatively insensitive to the assumed shape of the spectrum (e.g., Maloney et al. 1996). As these models

demonstrate, strong X-ray irradiation leads to decreased abundances of molecular species such as HCN and C<sub>2</sub>H<sub>2</sub>. These results are consistent with earlier studies (e.g. Lepp & Dalgarno 1996) which show an initial increase in the HCN abundance with increasing ionization rate ( $\xi/n_{\text{H}}$  up to  $10^{-18} \text{ cm}^{-3} \text{ s}^{-1}$ ) but then an effectively complete destruction of HCN for  $\xi/n_{\text{H}} \gtrsim 10^{-17} \text{ cm}^{-3} \text{ s}^{-1}$ . For comparison, the X-ray flux implied by a gas temperature of 200 K ( $\simeq 30 \text{ erg cm}^{-2} \text{ s}^{-1}$ ) corresponds to an ionization rate of  $5 \times 10^{-17} \text{ cm}^{-3} \text{ s}^{-1}$  at a density of  $10^6 \text{ cm}^{-3}$ . Clearly, the warm molecular gas revealed by these observations is inconsistent with strong X-ray illumination.

### 4.3. Static hot-core chemistry

At first sight our mid-infrared results resemble those toward a sample of massive Galactic young stellar objects (YSOs). For these, the molecular absorption features originate in the warm, dense gas near the newly formed star during the so-called hot core phase (Boonman et al. 2003; Lahuis & van Dishoeck 2000; Lacy et al. 1989; Evans et al. 1991). This is generally thought to represent a very early phase ( $\Delta t \leq 10^5 \text{ yr}$ ) in the formation of massive stars, during the transition from the deeply embedded stage to the phase where ionizing photons can escape the protostellar accretion envelope and create first a hyper- and later an ultra-compact HII region (see review by Cesaroni 2005). The molecular composition of the hot core is very different from that of cold molecular clouds. This is thought to reflect the evaporation of ices – resulting from accretion and surface chemistry during the cold preceding dark cloud phase – when the envelope is heated by the newly formed star (Walmsley & Schilke 1993). Subsequent high temperature gas-phase chemistry significantly enhances the abundance of e.g. CH<sub>4</sub>, C<sub>2</sub>H<sub>2</sub> and HCN up to three orders of magnitude, compared to cold dense molecular cloud abundances, for the most evolved sources (Viti & Williams 1999; Doty et al. 2002; Rodgers & Charnley 2003).

In Figure 4 the observed abundances and abundance ratios toward the (U)LIRGs are compared to those of a sample of Galactic massive YSOs. Both the YSO and the (U)LIRG sample show comparable, large variations in gas temperature and abundances. However, the HCN and C<sub>2</sub>H<sub>2</sub> abundances show a positive correlation with the gas temperature for the YSO sample but not for the (U)LIRG sample. Indeed, at low temperatures ( $< 400 \text{ K}$ ), the (U)LIRG abundances are some two orders of magnitude larger than those in YSO spectra.

For the Galactic YSOs, the observed correlation between the excitation temperature and the observed abundances (Figure 4) are in fair agreement with chemical models for such regions (Stäuber et al. 2005). The absence of a similar temperature correlation for (U)LIRGs may reflect a systematic (and large) error in the abundance determination (Section 3.3) or it may reflect a true difference between the chemical or physical evolution of the warm gas of the YSOs and (U)LIRGs. In this respect, we note that the C<sub>2</sub>H<sub>2</sub>/HCN ratio for both samples are very similar, however the

$\text{CO}_2/\text{HCN}$  and  $\text{CO}_2/\text{C}_2\text{H}_2$  ratios are reduced for the (U)LIRG sample up to an order of magnitude. If static steady-state hot-core chemistry were to apply to the (U)LIRGs as it does to the YSOs,  $\text{CO}_2$  would have been detected toward most of the sources in our sample. The fact it has not, suggests that a different chemistry may apply to the warm molecular gas in these (U)LIRGs.

#### 4.4. Pressure confined starburst chemistry

Static steady-state hot-core and X-ray chemical models have difficulties to consistently reproduce the observed high abundances of warm  $\text{C}_2\text{H}_2$  and HCN gas and low abundance of  $\text{CO}_2$  gas for most of our (U)LIRG sample. Essentially, static chemistry has a hard time producing high abundance of HCN and  $\text{C}_2\text{H}_2$  in the warm (100–400 K) gas characteristic for most of our (U)LIRG sample, while at the same time reducing the  $\text{CO}_2$  abundance. One possible solution to this conundrum is to produce high  $\text{C}_2\text{H}_2$  and HCN, and low  $\text{CO}_2$  abundances in hot gas ( $\gtrsim 800$  K), and then transport it outward to the cooler gas on a dynamical timescale which is rapid compared to the chemical timescale. At high temperatures, the hydrocarbon and nitrogen chemistry are enhanced as most of the oxygen is converted into water by neutral-neutral reactions. The abundances of molecules such as  $\text{C}_2\text{H}_2$ ,  $\text{CH}_4$ , and HCN can be increased by orders of magnitude (e.g. Doty et al. 2002; Rodgers & Charnley 2003) while at the same time the formation of  $\text{CO}_2$  is reduced as its primary formation route through OH is blocked. For cold Galactic molecular clouds, the chemical timescale is set by the cosmic ray ionization rate and is about  $3 \times 10^5$  yr, independent of density (Glassgold & Langer 1973). In a (U)LIRG (or AGN) environment, the cosmic ray flux may be increased considerably, shortening this timescale. Likewise, neutral-neutral reaction channels may open up in warm gas, further reducing the chemical timescale. In any case, these timescales are much shorter than the evolutionary timescale of massive stars or of the starburst. With the typical sizescale of the warm molecular zone ( $\sim 3 \times 10^{16}$  cm), a timescale of  $3 \times 10^5$  yr translates into a ‘diffusion’ velocity of only  $0.03 \text{ km s}^{-1}$ . Even a 100 times faster chemical timescale only requires a ‘diffusion’ velocity of a few  $\text{km s}^{-1}$ . Since the chemical models are well capable of explaining high abundances for both  $\text{C}_2\text{H}_2$  and HCN and a low abundance for  $\text{CO}_2$  at high temperatures and densities, and in light of the discussion above, this ‘mixing’ is attributed to the global activity created by pressure confined massive starburst activity. The strong gravitational potential in the nuclei of these galaxies inhibits the disruption of the surrounding warm molecular envelopes by HII regions and supernovae, while producing sufficient turbulent (or wind) motion to distribute warm  $\text{C}_2\text{H}_2$ - and HCN-rich and  $\text{CO}_2$ -poor gas in the colder outer envelope regions.

## 5. Summary

We have observed the absorption lines due to the *Q*-branch transitions of C<sub>2</sub>H<sub>2</sub>, HCN, and CO<sub>2</sub> in the mid-IR spectra of a large number of (U)LIRGs. These observations reveal for the first time the presence of copious amounts of warm (200–700 K), dense ( $n > 10^7$  cm<sup>−3</sup>) molecular gas in these nuclei. The origin of this warm molecular gas is unclear. Theoretical models show that the X-ray fluxes implied by the elevated gas temperatures rapidly destroy these molecules and hence it is unlikely that this warm molecular gas is associated with a dense toroid surrounding an active central engine. Warm, dense gas rich in C<sub>2</sub>H<sub>2</sub>, HCN, and CO<sub>2</sub> is commonly observed towards galactic massive protostars and is associated with a short-lived phase – the Hot Core phase – before advancing ionization fronts disrupt the core. The high molecular abundances in galactic Hot Cores are well understood chemically. However, the derived abundances of C<sub>2</sub>H<sub>2</sub> and HCN for the cooler (U)LIRGs ( $T_{\text{ex}} \simeq 200–400$  K) in our sample as well as the C<sub>2</sub>H<sub>2</sub>/CO<sub>2</sub> and HCN/CO<sub>2</sub> ratios are very different from those in galactic protostars. We suggest that this warm molecular gas is associated with a phase of deeply embedded star formation in (U)LIRGs where the high pressures and densities have inhibited the disruption of the star forming, molecular cores by prohibiting the expansion of HII regions, trapping the star formation process in an extended Hot-Core phase. The chemical differences between these (U)LIRGs and galactic Hot Cores may then reflect enhanced mixing between warm and cold phases due to the high degree of turbulence or wind motion associated with extreme starburst environments. Pressure confined massive starburst activity may thus be the driving energy source behind the observed C<sub>2</sub>H<sub>2</sub> and HCN rich warm molecular gas and responsible for most of the near-IR characteristics of the deeply obscured (U)LIRGs.

The current analysis is predominately based on the observed abundances derived from moderate resolution, mid-IR vibration-rotation absorption bands of C<sub>2</sub>H<sub>2</sub> and HCN. This analysis can be extended using high resolution, velocity resolved, ground-based studies of the *P*- and *R* branches of these molecules as well as from the  $\nu = 1 - 0$  rotation-vibration band of CO. In addition, observations of more molecular rotation-vibration bands and high excitation submillimeter lines of a large sample of molecules may be instrumental for progress in this field. Specifically, velocity and spatially resolved infrared and millimeter data can constrain the source morphology. In combination with optimized physicochemical models for individual sources it may become possible to draw firm conclusions about the physical characteristics of the warm molecular gas and the true nature of the power sources in the (U)LIRG nuclei.

The authors would like to thank Tom Geballe for sharing early results and the CO data of IRAS 08572+3915NW; John Lacy and Claudia Knez for sharing the TEXES data; and Bernhard Brandl, Kees Dullemond, Masa Imanishi, David Rupke, and Marco Spaans for many useful discussions. Astrochemistry in Leiden is supported by a Spinoza grant from NWO.

## REFERENCES

Aalto S. 2005, in IAU Symposium 231, ed. Dariusz, C. L., Geoffrey, A. B., & Eric, H. (Cambridge University Press), 261

Armus, L. and Heckman, T. M., & Miley, G. K. 1987, AJ, 94, 831

Armus, L. and Heckman, T. M., & Miley, G. K. 1989, ApJ, 347, 727

Armus, L., et al. 2004, ApJS, 154, 178

Armus, L., et al. 2006, ApJ, 640, 204

Armus, L., et al. 2006, ApJ, (in press atro-ph/0610218)

Bergin, E. A. and Langer, W. D. 1997, ApJ, 486, 316

Boonman, A.M.S., van Dishoeck, E.F, Lahuis, F., & Doty, S.D. 2003, A&A, 399, 1063

Cesaroni, R. 2005, in IAU Symposium 227, ed. Cesaroni, R., Felli, M., Churchwell, E., & Walmsley, M. (Cambridge University Press), 59

Darling, J., & Giovanelli, R. 2002, AJ, 124, 100

Decin, L., Morris, P. W., Appleton, P. N., Charmandaris, V., Armus, L., & Houck, J. R. 2004, ApJS, 154, 408

Doty, S.D., van Dishoeck, E.F., van der Tak, F.F.S., & Boonman, A.M.S. 2002, A&A, 389, 446

Downes, D. & Solomon, P. M. 1998, ApJ, 507, 615

Evans, N. J., Lacy, J. H., & Carr, J. S. 1991, ApJ, 383, 674

Gao, Y. & Solomon, P. M. 2004, ApJ, 606, 271

Geballe, T. R., Goto, M., Usuda, T., Oka, T., McCall, B. J. 2006, ApJ, 644, 907

Genzel, R. & Cesarsky, C.J. 2000, ARA&A, 38, 761

Glassgold, A. E. & Langer, W. D. 1973, ApJ, 179, 147

Houck, J. R., et al. 2004, ApJS, 154, 18

Imanishi M., Nakanishi, K., & Kohno, K. 2006, AJ, 31, 2888

Lacy, J., et al. 2002, PASP, vol. 114, 153

Kessler-Silacci, J., et al. 2006, *ApJ*, 639, 275

Kim, D.-C. & Sanders, D. B. 1998, *ApJS*, 119, 41

Kohno, K. 2005 in AIP 783: The Evolution of Starbursts, ed. Hüttmeister, S., Manthey E., Bomans, D., & Weis, K. (AIP Conference Proceedings), 203 (astro-ph/0508420)

Lacy, J. H., Evans, N. J., Achtermann, J. M., Bruce, D. E., Arens, J. F., & Carr, J. S. 1989 *ApJ*, 342, L43

Lahuis, F., & van Dishoeck, E. F. 2000, *A&A*, 355, 699

Lahuis, F. and Boogert, A. 2003, in SFChem 2002: Chemistry as a Diagnostic of Star Formation, ed. C. L. Curry and M. Fich. (NRC Press, Ottawa, Canada), 2003, 335.

Lahuis, F. et al. 2006, “c2d Spectroscopy Explanatory Supplement”, (Pasadena: *Spitzer* Science Center)

Lepp, S. & Dalgarno, A. 1996, *A&A*, 306, L21

Low, F. J., Cutri, R. M., Huchra, J. P., & Kleinmann, S. G. 1988, *ApJ*, 327, 41

Maloney, P. R., Hollenbach, D. J., & Tielens, A. G. G. M. 1996, *ApJ*, 466, 561

Meijerink, R., & Spaans, M. 2005, *A&A*, 436, 397

Mihos, J. C., & Hernquist, L. 1996, *ApJ*, 464, 641

Mitchell, G. F., Maillard, J.-P., Allen, M., Beer, R., & Belcourt, K. 1990, *ApJ*, 363, 554

Murphy, T. W., Armus, L., Matthews, K., Soifer, B. T., Mazzarella, J. M., Shupe, D. L., Strauss, M. A., & Neugebauer, G. 1996, *AJ*, 111, 1025

Roche, P. F., & Aitken, D. K. 1984, *MNRAS*, 208, 481

Roche, P. F., & Aitken, D. K. 1985, *MNRAS*, 215, 425

Rodgers, S.D., & Charnley, S.B. 2003, *ApJ*, 585, 355

Sanders, D. B., Soifer, B. T., Elias, J. H., Neugebauer, G., & Matthews, K. 1988, *ApJ*, 328, 35

Sanders, D. B., Soifer, B. T., Elias, J. H., Madore, B. F., Matthews, K., Neugebauer, G., & Scoville, N. Z. 1988, *ApJ*, 325, 74

Solomon, P. M., Downes, D., Radford, S. J. E., & Barrett, J. W. 1997, *ApJ*, 478, 144

Spoon, H. W. W., Armus, L., Cami, J., Tielens, A. G. G. M., Chiar, J. E., Peeters, E., Keane, J. V., Charmandaris, V., Appleton, P. N., Teplitz, H. I., & Burgdorf, M. J. 2004, *ApJS*, 154, 184

Spoon, H. W. W., Keane, J. V., Cami, J., Lahuis, F., Tielens, A. G. G. M., Armus, L., & Charmandaris, V. 2006, in *IAU Symposium 231*, ed. Dariusz, C. L., Geoffrey, A. B., & Eric, H. (Cambridge University Press), 281

Spoon, H. W. W., Tielens, A. G. G. M., Armus, L., Sloan, G. C., Sargent, B., Cami, J., Charmandaris, V., Houck, J. R., & Soifer, B. T. 2006, *ApJ*, 638 759

Spoon H. W. w., Marshall, J. A., Houck, J. R., Elitzur M., Hao, L., Armus, L., Brandl, B. R., & Charmandaris, V., *ApJL* (astro-ph/0611918)

Stanford, S. A., Stern, D., van Breugel, W. & De Breuck, C. 2000, *ApJS*, 131, 185

Stäuber, P., Doty, S. D., van Dishoeck, E. F., & Benz, A. O., 2005, *A&A*, 440, 949

Stäuber, P., Benz, A. O., Jørgensen, J. K., van Dishoeck, E. F., Doty, S. D., & F. F. S. van der Tak, *A&A*, (astro-ph/0608393)

Strauss, M. A., Huchra, J. P., Davis, M., Yahil, A., Fisher, K. B. & Tonry, J. 1992, *ApJS*, 83, 29

Veilleux, S., Kim, D.-C., Sanders, D. B., Mazzarella, J. M., & Soifer, B. T. 1995, *ApJS*, 98, 171

Veilleux, S., Goodrich, R. W., & Hill, G. J. 1997, *ApJ*, 477, 631

Viti, S., & Williams, D. A. 1999, *MNRAS*, 305, 755

Walmsley, C. M., & Schilke, P. 1993, in *Dust and Chemistry in Astronomy*, ed. Millar T.J., & Williams, D.A. (IOP Publishing, Bristol), 37

Werner, M., et al. 2004, *ApJS*, 54, 1

Table 1. Observation details and basic source properties

Target	AOR Key	Pipeline	Observed	Integration Time <sup>a</sup> (sec)	$z$	$\log L_{\text{IR}}$ ( $L_{\odot}$ )	$\tau_{9.7}$	Optical/Near-IR Class <sup>b</sup>	$D_L$ <sup>c</sup> (Mpc)
17208-0014	4986624	S12.0.2	27 Mar 2004	$31 \times 6 \times 2$	0.0430	12.46	1.9	H II	188
Arp 220	4983808	S12.0.2	29 Feb 2004	$31 \times 6 \times 2$	0.0181	12.17	3.3	LINER <sup>1</sup>	78
IC 860	6652416	S13.2.0	10 Feb 2005	$121 \times 2 \times 2$	0.0112	10.96	2.1		48
22491-1808	4990976	S13.2.0	24 Jun 2004	$121 \times 2 \times 2$	0.0773	12.19	1.1	Starburst <sup>2,3</sup>	346
NGC 4418	4935168	S13.2.0	8 Jul 2005	$31 \times 6 \times 2$	0.0073	11.03	4.4		31
13218+0552	4979200	S13.2.0	17 Jul 2004	$121 \times 3 \times 2$	0.2051	12.71	0.8	QSO/Sey-1 <sup>4,5</sup>	998
15250+3609	4983040	S12.0.2	4 Mar 2004	$31 \times 6 \times 2$	0.0554	12.05	3.8		244
05189-2524	4969216	S13.2.0	22 Mar 2004	$31 \times 6 \times 2$	0.0426	12.19	0.4	Seyfert-2/1 <sup>6</sup>	186
Mrk 231	4978688	S13.2.0	14 Apr 2004	$31 \times 6 \times 2$	0.0422	12.52	0.8	Seyfert-1 <sup>2</sup>	184
Mrk 273	4980224	S12.0.2	14 Apr 2004	$31 \times 6 \times 2$	0.0378	12.15	1.9	Seyfert-2	164
00397-1312	4963584	S12.0.2	4 Jan 2004	$121 \times 3 \times 2$	0.2617	12.90	3.3		1317
20100-4156	4989696	S13.2.0	13 Apr 2004	$121 \times 2 \times 2$	0.1296	12.65	3.3		601
UGC 5101	4973056	S13.2.0	23 Mar 2004	$31 \times 6 \times 2$	0.0400	12.00	1.7	LINER <sup>3</sup>	164
01003-2238	4972032	S12.0.2	4 Jan 2004	$121 \times 2 \times 2$	0.1177	12.29	0.7	Seyfert-2 <sup>1</sup>	542
08572+3915	4972032	S13.2.0	15 Apr 2004	$31 \times 6 \times 2$	0.0584	12.10	4.2	LINER <sup>1</sup>	258
02530+0211	6652160	S13.2.0	10 Feb 2005	$31 \times 3 \times 2$	0.0276	11.04	3.7		119
12112+0305	4977664	S13.2.0	4 Jan 2004	$121 \times 2 \times 2$	0.0727	12.33	1.3	LINER <sup>1</sup>	324
14348-1447	4981248	S13.2.0	7 Feb 2004	$121 \times 2 \times 2$	0.0827	12.35	2.1	LINER <sup>2</sup>	372
NGC 6240	4985600	S13.2.0	4 Mar 2004	$31 \times 6 \times 2$	0.0245	11.84	1.2	LINER	119

<sup>a</sup>Ramp integration time  $\times$  number of cycles  $\times$  number of slit positions<sup>b</sup>Optical/NIR spectral classifications taken from: (1) Armus, Heckman, & Miley (1989), (2) Sanders et al. (1988b), (3) Veilleux et al. (1995), (4) Low et al. (1988), (5) Darling & Giovanelli (2002), (6) Veilleux, Goodrich, & Hill (1997)<sup>c</sup>assuming  $H_0 = 71 \text{ km s}^{-1} \text{ Mpc}^{-1}$ ,  $\Omega_M = 0.27$ ,  $\Omega_\Lambda = 0.73$ ,  $\Omega_K = 0$

Table 2. LTE excitation parameters and spectral characteristics

Target	$T_{\text{ex}}^{\text{a}}$ (K)	$N_{\text{C}_2\text{H}_2}^{\text{a}}$ ( $10^{16}\text{cm}^{-2}$ )	$N_{\text{HCN}}^{\text{a}}$ ( $10^{16}\text{cm}^{-2}$ )	$N_{\text{CO}_2}^{\text{a}}$ ( $10^{16}\text{cm}^{-2}$ )	$N_{\text{H}_2}$ ( $10^{22}\text{cm}^{-2}$ )	$x_{\text{C}_2\text{H}_2}^{\text{b}}$ ( $10^{-8}$ )	$x_{\text{HCN}}^{\text{b}}$ ( $10^{-8}$ )	$x_{\text{CO}_2}^{\text{b}}$ ( $10^{-8}$ )	cont <sup>c</sup> (Jy)	SNR <sup>d</sup>
17208-0014	230	0.6	1.2	< 0.2	3.3	18	36	< 6	0.20	200
Arp 220	250	1.7	2.9	0.7	5.8	29	50	12	0.93	150
IC 860	280	3.1	7.2	0.9	3.7	84	195	24	0.09	150
22491-1808	280	1.0	1.4	< 0.3	1.9	53	74	< 16	0.07	130
NGC 4418	300	5.3	12.	< 0.4	7.7	69	156	< 5	2.34	150
13218+0552	300	0.4	1.5	< 0.5	1.4	28	107	< 36	0.26	180
15250+3609	320	4.7	7.0	0.7	6.7	70	105	10	0.27	90
05189-2524	350	0.4	1.5	0.8	0.7	57	214	114	1.05	200
Mrk 231	410	0.6	1.4	< 0.4	1.4	43	100	< 29	2.83	200
Mrk 273	510	0.9	1.7	< 0.4	3.3	27	52	< 12	0.37	200
00397-1312	540	0.6	3.0	< 0.4	5.8	10	52	< 7	0.12	150
20100-4156	560	3.8	8.9	< 0.9	5.8	66	153	< 15	0.11	70
UGC 5101	590	1.0	2.2	< 0.5	3.0	33	73	< 17	0.24	130
01003-2238	630	0.5	1.3	< 0.8	1.2	42	108	< 67	0.27	200
08572+3915	700	2.4	3.7	< 0.5	7.4	32	50	< 7	0.74	150
02530+0211	300 <sup>e</sup>	< 0.5	< 3	< 0.3	6.5	< 8	< 46	< 5	0.25	100
12112+0305	300 <sup>e</sup>	< 0.8	< 2.3	< 0.6	3.0	< 27	< 77	< 20	0.07	150
14348-1447	300 <sup>e</sup>	< 0.5	< 1	< 0.2	3.7	< 14	< 27	< 5	0.07	80
NGC 6240	300 <sup>e</sup>	< 0.2	< 0.7	< 0.6	2.1	< 10	< 33	< 29	0.68	100

<sup>a</sup>The excitation temperature is poorly constrained and can be uncertain up to 30%. See Section 3.2 and Figure 2 for details.

<sup>b</sup>Abundances wrt.  $\text{H}_2$  assuming  $N_{\text{H}} = \tau_{9.7}(3.5 \times 10^{22})\text{cm}^{-2}$  and  $N_{\text{H}} = 2 \times N_{\text{H}_2}$  (see Section 3.3).

<sup>c</sup>Continuum at 14  $\mu\text{m}$  in the rest wavelength frame.

<sup>d</sup>Signal to Noise Ratio (SNR) estimated from the residuals after subtraction of the synthetic spectrum. It varies over the covered wavelength range.

<sup>e</sup>Temperature fixed to 300 K for derivation of column density upper limit estimates.

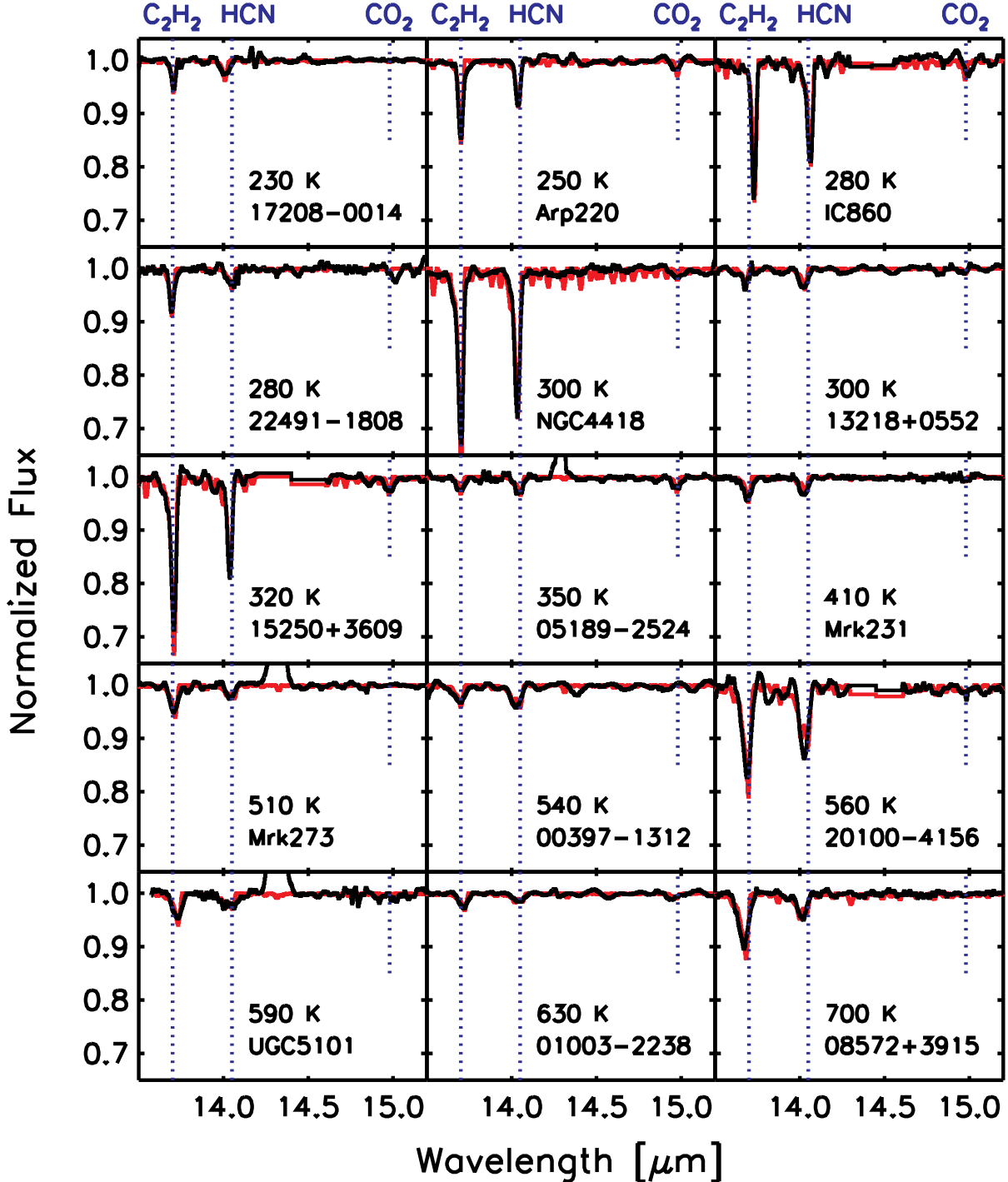


Fig. 1.— Continuum divided *Spitzer*-IRS spectra of a sample of (U)LIRGs showing the absorption bands of  $\text{C}_2\text{H}_2$  and HCN and some of  $\text{CO}_2$ . Plotted in red are best-fit synthetic spectra assuming a single excitation temperature for all three molecules. All spectra have been shifted to the rest wavelengths.

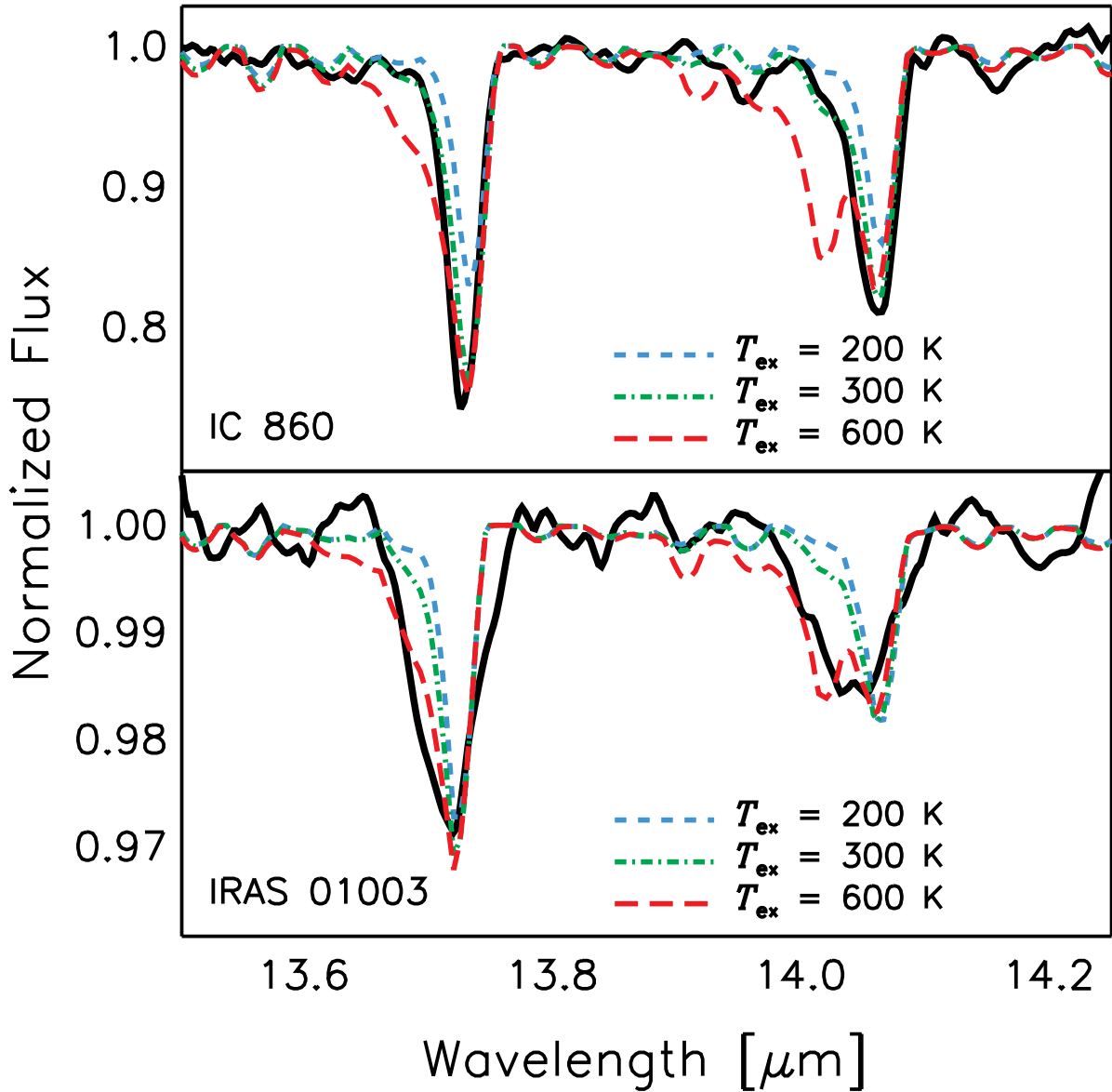


Fig. 2.— Illustration of the temperature sensitivity of the  $\text{C}_2\text{H}_2$  and HCN  $Q$ -branch profiles in direct comparison to the observed spectra of IC 860 (best fit  $T_{\text{ex}} = 280$  K) and IRAS 01003-2238 (best fit  $T_{\text{ex}} = 630$  K). The shape of the  $Q$ -branch profile determines the derived excitation temperatures with an uncertainty of  $\sim 30\%$ . A better constrained error estimate is difficult to determine at the IRS resolution.

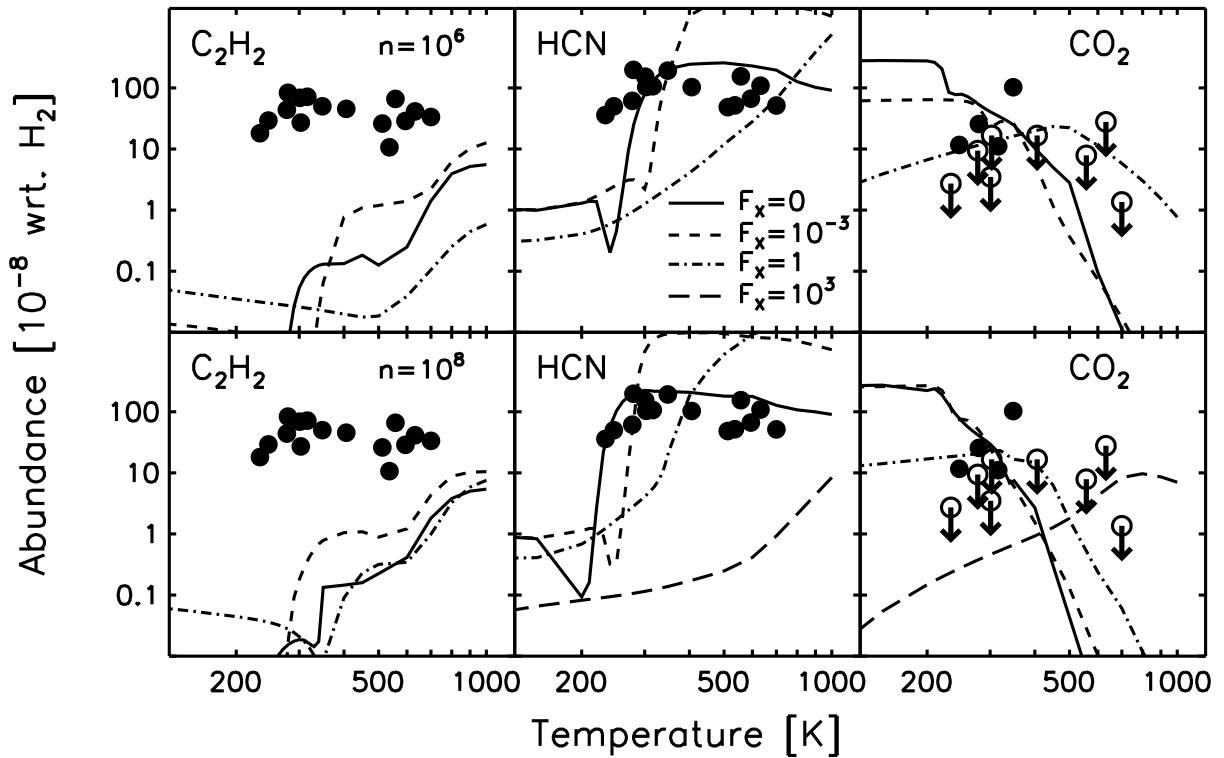


Fig. 3.— Results of equilibrium X-ray enhanced chemical models for the three observed molecules. The calculated abundances are shown for moderate ( $10^6 \text{ cm}^{-3}$ ) and high density ( $10^8 \text{ cm}^{-3}$ ) and four X-ray flux levels ( $F_X = 0, 10^{-3}, 1$  and  $10^3 \text{ erg cm}^{-2} \text{ s}^{-1}$ ) plotted with solid, dashed, dot-dashed, and long-dashed lines). Note that except for HCN and CO<sub>2</sub> at high density, the abundances for the highest X-ray flux are below the plotted range. Overplotted are the observed abundances. Details of the model can be found in Stäuber et al. (2005, 2006).

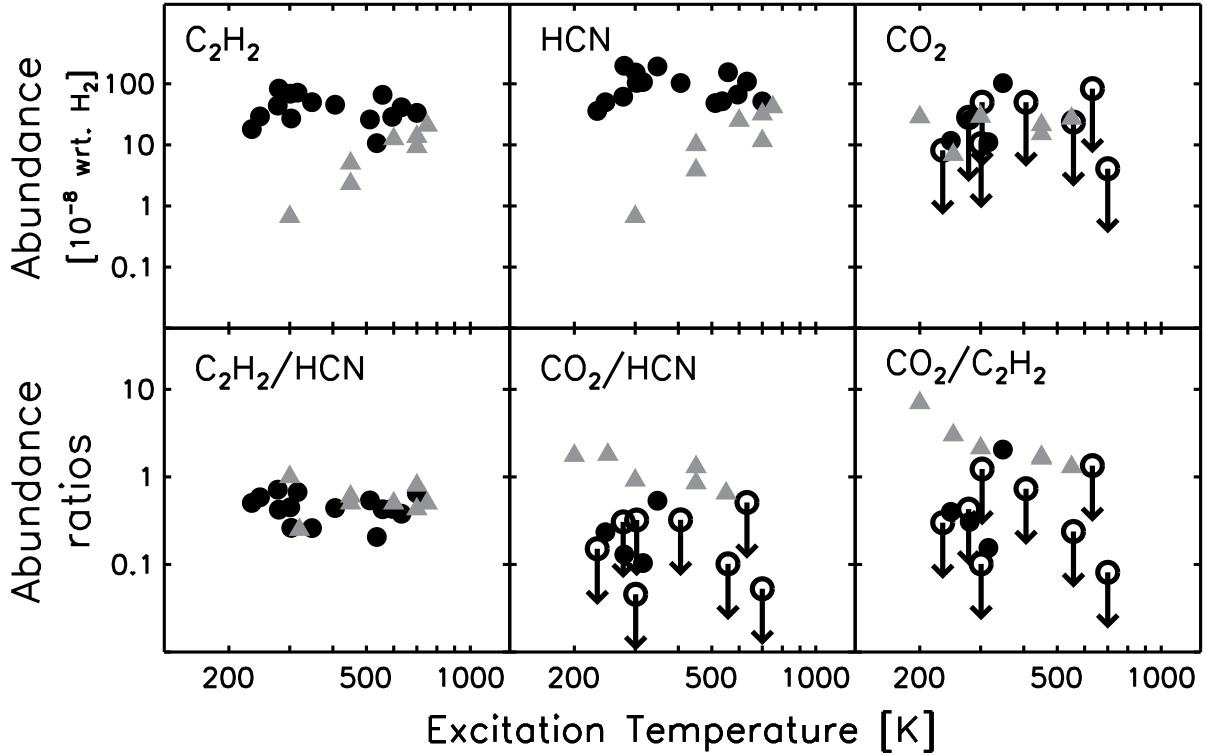


Fig. 4.— Top: observed  $\text{C}_2\text{H}_2$ , HCN and  $\text{CO}_2$  abundances using a total  $\text{H}_2$  column obtained from the  $9.8\mu\text{m}$  silicate absorption band. Bottom: abundance ratios of  $\text{C}_2\text{H}_2$ , HCN and  $\text{CO}_2$ . Both the absolute abundances and the abundance ratios are indicated with circles and are presented as functions of excitation temperature. Included are the observed values toward a sample of Galactic massive YSOs (Boonman et al. 2003; Lahuis & van Dishoeck 2000) plotted with grey triangle symbols. The derived absolute abundances toward the (U)LIRGs show significant enhancements in the abundances of  $\text{C}_2\text{H}_2$  and HCN for sources with excitation temperatures below 500 K. The  $\text{C}_2\text{H}_2/\text{HCN}$  abundance ratios are quite similar, however the  $\text{CO}_2/\text{C}_2\text{H}_2$  and  $\text{CO}_2/\text{HCN}$  ratios toward the (U)LIRGs are systematically lower than toward the Galactic massive YSOs suggesting that a different chemistry may apply.